

Synthesis and Voltage-Clamp Studies of Methyl 1,4-Dihydro-2,6-dimethyl-5-nitro-4-(benzofurazanyl)pyridine-3-carboxylate Racemates and Enantiomers and of Their Benzofuroxanyl Analogues

Sonja Visentin,[†] Pascale Amiel,[†] Roberta Fruttero,[†] Donatella Boschi,[†] Christian Roussel,[§] Laura Giusta,[‡] Emilio Carbone,[‡] and Alberto Gasco^{*,†}

Department of Scienza e Tecnologia del Farmaco, Facoltà di Farmacia, Università degli Studi di Torino, via P. Giuria 9, 10125 Torino, Italy, Department of Neuroscienze, Unità di ricerca INFM, Università degli Studi di Torino, Corso Raffaello 30, 10125 Torino, Italy, and ENSSPICAM, University Aix Marseille III, Av. Escadrille Normandie Niemen, F-13397 Marseille Cedex 20, France

Received November 4, 1998

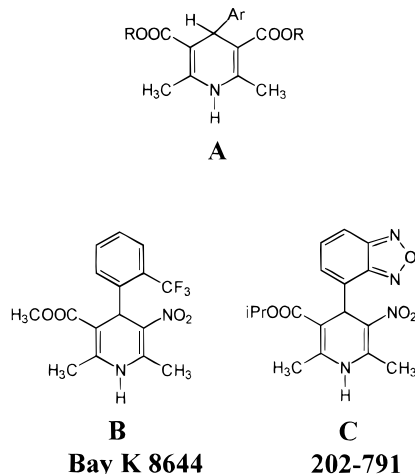
Racemic methyl 1,4-dihydro-2,6-dimethyl-5-nitro-4-(benzofurazanyl)pyridine-3-carboxylates (\pm)-**10** and (\pm)-**11** and their benzofuroxanyl analogues (\pm)-**12** and (\pm)-**13** were prepared using a modified Hantzsch reaction that involved the condensation of nitroacetone with methyl 3-aminocrotonate and the appropriate aldehydes. The racemic mixtures were resolved into the corresponding enantiomers. Whole-cell voltage-clamp studies on L-type Ca^{2+} channels expressed in a rat insulinoma cell line (RINm5F) showed that all the dextrorotatory antipodes were effective agonists of L-type Ca^{2+} currents, while the levorotatory ones were weak Ca^{2+} entry blockers. The (+)-enantiomer of benzofurazan-5'-yl derivative **11** demonstrated unusual activity in that, in addition to producing a potentiation of L-type currents, it interfered with the voltage-dependent gating of L-type channels by producing a net delay of their activation at low voltages. This compound represents an interesting tool to probe L-type Ca^{2+} channel structure and function.

Introduction

1,4-Dihydropyridines (DHPs) are an important class of drugs which exert potent blocking activities on calcium (Ca^{2+}) currents through voltage-dependent L-type channels.¹ Several DHPs are clinically used in the treatment of a number of cardiovascular diseases. Classical 1,4-dihydropyridines have the structure A (Chart 1). Structure–activity relationships of this class of compounds have been the subject of several studies.^{1,2} The ester groups in the 3- and 5-positions are of crucial importance for activity. If one of the two ester moieties is replaced by appropriate groups such as nitro, lactone, and thiolactone, the symmetry of the molecule is lost and the resulting derivative exists as a pair of enantiomers, which have opposite pharmacological profiles. Indeed one of the antipodes is a calcium entry blocker (calcium antagonist), while the other is a calcium entry activator (calcium agonist).^{1–3} Classical examples of this behavior are the two enantiomeric pairs Bay K8644 (B) and 202-791 (C) (Chart 1). Ca^{2+} channel activators are interesting pharmacological tools. They represent potential new drugs for the management of congestive heart failure, in view of their positive inotropic effects. Derivatives able to act as dual cardioselective calcium channel agonists and smooth muscle-selective calcium channel antagonists would be of great utility for the treatment of cardiovascular diseases.⁴

In a recent paper we reported the synthesis, structure, and calcium entry blocker activity of a number of

Chart 1



benzofurazanyl- and benzofuroxanyl-1,4-dihydropyridines.⁵ All the compounds displayed potent calcium antagonist properties, evaluated in isolated rabbit basilar artery by measuring relaxation of calcium-induced contractions in high K^{+} -depolarizing solutions. The activity of benzofurazan derivatives was not substantially changed by N-oxidation. On these grounds, as a logical progression of our work on benzofurazanyl- and benzofuroxanyl-1,4-dihydropyridines, we synthesized derivatives **10–13** (Chart 2) and studied the action of the racemic mixtures and the single enantiomers on L-type Ca^{2+} channels expressed by a rat insulinoma cell line (RINm5F cells). Here we show that this class of molecules, besides causing the typical Ca^{2+} current enhancement of 1,4-DHP agonists, is also able to interfere with the activation kinetics of L-type channels,

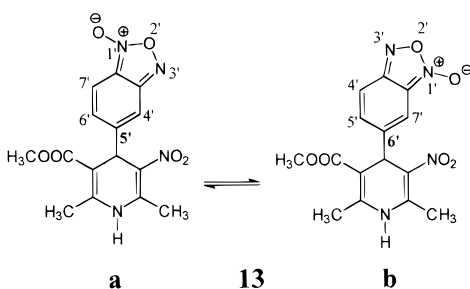
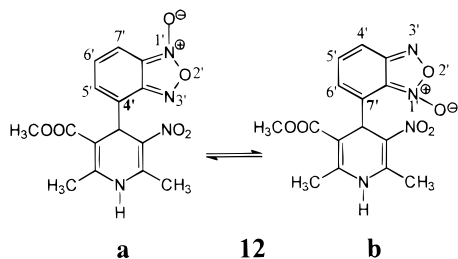
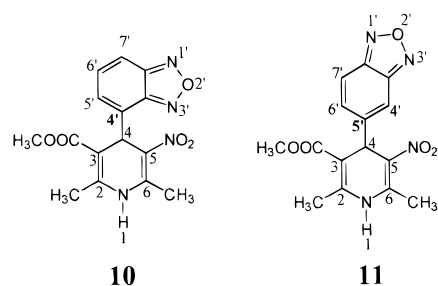
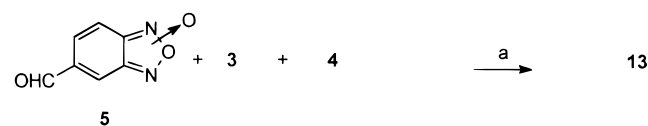
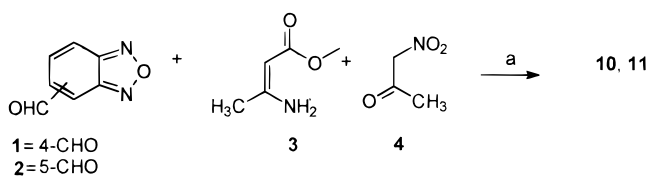
* To whom correspondence should be addressed. Phone: 0039-11-6707670. Fax: 0039-11-6707659. E-mail: gasco@pharm.unito.it.

[†] Department of Scienza e Tecnologia del Farmaco.

[‡] Department of Neuroscienze.

[§] ENSSPICAM.

Chart 2

Scheme 1^a

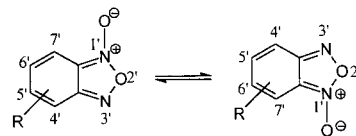
^a (a) iPrOH, Δ.

suggesting specific interactions with the charged groups of the protein responsible for the voltage dependence of channel opening. These compounds may represent an interesting new class of drugs for probing L-type Ca²⁺ channel structure and function.

Results

Chemistry. The racemic methyl 1,4-dihydro-2,6-dimethyl-5-nitro-4-(benzofurazan-4-yl)pyridine-3-carboxylate (**10**) and the benzofurazan-5-yl analogue **11** were prepared by a modified Hantzsch reaction. The condensation of nitroacetone (**4**) with methyl 3-aminocrotonate (**3**) and either 4-benzofurazan-2-carbaldehyde (**1**) or 5-benzofurazan-2-carbaldehyde (**2**) afforded the expected compounds in fair yield (Scheme 1). ¹H NMR spectra are in agreement with the proposed structures. Synthesis and structural characterization of benzofuroxan derivatives **12** and **13** require more detailed consideration. It is

A)



B)

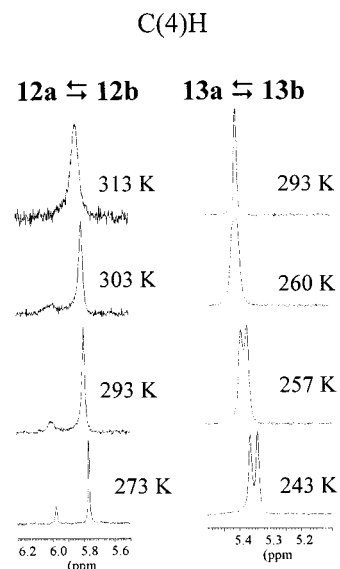
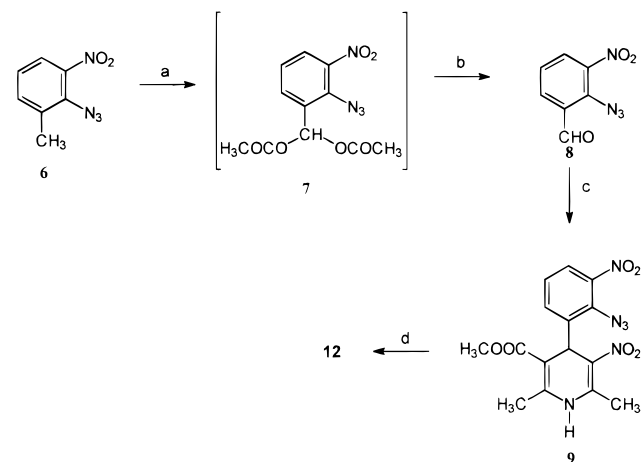


Figure 1. Temperature dependence of the C(4)H 1,4-DHP protons of **12** and **13**.

Scheme 2^a

^a (a) CH₃COOH, Thiele reagent (CrO₃, (CH₃CO)₂O, H₂SO₄); (b) EtOH, HCl; (c) iPrOH, **3**, **4**, Δ; (d) *hν*, 24 h, distilled THF.

known that substituted benzofuroxans exhibit the isomerization (or tautomerism) equilibrium (Figure 1A). Depending on both the nature and the position of R substituents, as well as on the solvent and the temperature, the equilibrium can assume different positions.^{6,7} The racemic methyl 1,4-dihydro-2,6-dimethyl-5-nitro-4-(benzofuroxan-5(6)-yl)pyridine-3-carboxylate (**13**) was obtained in a manner similar to the benzofurazan-yl analogues **10** and **11** (Scheme 1).

Synthesis of derivative **12** required the more complex strategy shown in Scheme 2, since attempts to prepare it through the route used for the analogue **10** failed. The intermediate 2-azido-3-nitrobenzaldehyde (**8**) was obtained by oxidation of 2-azido-3-nitrotoluene (**6**), dissolved in acetic acid, with Thiele reagent (CrO₃-acetic

anhydride–H₂SO₄). The resulting 2-azido-3-nitrobenzal-diacetate (**7**) was hydrolyzed by hydrochloric acid to the expected aldehyde **8**. This latter compound was transformed into the desired methyl 1,4-dihydro-2,6-dimethyl-5-nitro-4-(2-azido-3-nitrophenyl)pyridine-3-carboxylate (**9**). Irradiation for 24 h of this derivative in distilled THF solution with a medium-pressure Hg lamp in an immersion well–photochemical apparatus afforded derivative **12** in fair yield.

The ¹H NMR spectra in CD₃COCD₃ of the two benzofuroxan DHPs, at room temperature, show broad peaks, indicating extensive benzofuroxan tautomerism. On cooling, the spectrum of derivative **12** sharpens into a complex trace in the aromatic region, while the two broad signals due to C(4)H 1,4-DHP protons were transformed into a sharp biased doublet at 5.99 and 5.78 ppm, the signal at higher field being the more intense (Figure 1B). This latter peak is attributed to the 4'-tautomer **12a**, for steric reasons.⁷ At 273 K the intensity ratio was 83:17. Therefore ΔG° value at 273 K for the **12a** \rightleftharpoons **12b** equilibrium is ca. 3.5 kJ/mol in favor of **12a**. The separation of the two peaks, which did not change on further cooling, was $\delta = 43$ Hz. Coalescence of these signals was observed at approximately 313 K (*T*_c). Because of the large difference in abundance of the two tautomers and the consequent difficulties in evaluating the coalescence temperature, it was impossible to obtain a reliable value for the free energy of activation ΔG^\ddagger . From the temperature at which separate spectra were observed, we believe that this energy is ca. 63–67 kJ/mol. On cooling, the other regions of the spectrum also sharpen and remain substantially unchanged. The spectrum of derivative **13** behaves similarly. On lowering the temperature, the aromatic region sharpens into a first-order trace and the broad signal at 5.40 ppm due to C(4)H 1,4-DHP protons is transformed into a sharp doublet at 5.36 and 5.33 ppm (Figure 1B). The higher field signal is tentatively attributed to the 6'-tautomer **13b**. At 243 K the intensity ratio was ca. 1:1, indicating a ΔG° value for benzofuroxan tautomerism close to zero. The separation of the two peaks, $\delta = 4.9$ Hz, did not change on further cooling. Coalescence of the signals was observed at 263 K (*T*_c), indicating a free energy of activation $\Delta G^\ddagger = 58.6$ kJ/mol for the **13a** \rightleftharpoons **13b** interconversion.

The separation of racemic mixtures of compounds **10**–**13** was successfully carried out by HPLC, using an amylose (*S*)-1-phenylethyl carbamate (Chiralpak AS) column,⁸ on analytical as well as semipreparative scales. The single enantiomers were obtained in 97–100% optical purity.

As expected, theoretical studies using an AM-1 Hamiltonian algorithm show the same conformational domain for all the compounds. For both substances two energy minimum rotamers are possible; the benzoheterocycle system is in a pseudoaxial position and orthogonal to the dihydropyridine flat boat ring. In one conformation the heteropentatomic ring lies on the same side as the C(4)H 1,4-DHP hydrogen, while in the other it is oriented on the opposite side. This picture is typical of 4-phenyl-1,4-dihydropyridines *ortho* or *meta* substituted at the phenyl ring.²

Voltage-Clamp Studies. The four racemates illustrated in Chart 2 and their single enantiomers were

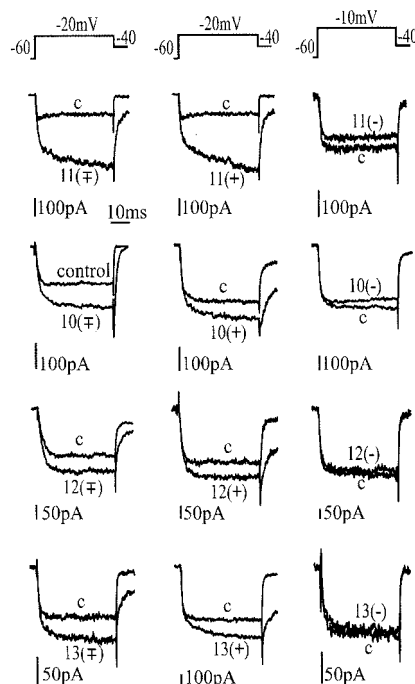


Figure 2. Action of benzofurazanyl- and benzofuroxanyl-1,4-DHPs on L-type Ba²⁺ currents of rat insulinoma RINm5F cells. Each panel consists of two current recordings: one control and one during application of the 1,4-DHP at 3 μ M concentration as indicated. The chemical structure of each racemate is drawn to the left. Pulse protocols are given at the head of each column. In the first and second column are reported the agonistic effects of the racemates and their (+)-enantiomers. On the third column are illustrated the antagonist effects of the (–)-enantiomers. Note the current enhancements at –20 mV and the prolonged tails at –40 mV induced by the agonists and the small antagonistic effects of the (–)-enantiomers. Each panel is obtained from a different RINm5F cell except for (±)-**11** and (+)-**11** which are from the same cell.

tested for their action on L-type Ca²⁺ channels expressed by the rat insulinoma cell line RINm5F.^{9,10} Cells were bathed in 10 mM Ba²⁺ and held at a relatively low resting potential (–60 mV) to increase the percentage of available L-type channels. Under these conditions, saturating concentrations of nifedipine (3 μ M) reversibly blocked about 70% of the total Ba²⁺ current ($66.7 \pm 2.8\%$, *n* = 14), indicating a predominance of L-over the non-L-type channels in these cells.

Figure 2 summarizes the typical action of the various DHPs on the Ba²⁺ currents of RINm5F cells when the compounds were applied at the same concentration (3 μ M). The test potential was –20 mV for the molecules with agonistic effects and –10 mV for those with antagonistic action. These conditions were chosen since –20 mV represents a membrane potential at which the open probability of L-type channels is sufficiently high to reveal maximal agonistic effects of the 1,4-DHPs, while –10 mV is a potential value that gives maximal activation for the L-type channel and is thus sufficiently high to test the blocking action of the antagonists. To better visualize the agonistic effects of the compounds, the return potential from test was set at –40 mV, which was sufficiently negative to produce fast decaying tail currents at control and slow tails with the agonist. As shown in Figure 2, all four racemates produced a current increase at –20 mV and a remarkable slowing of tail currents on return to –40 mV (left column). The

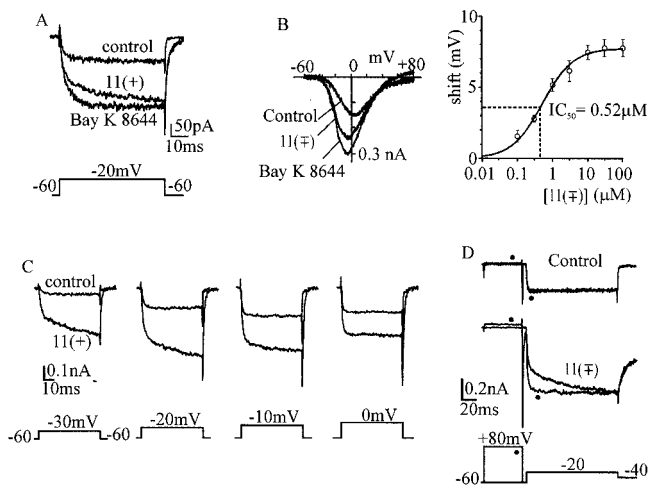


Figure 3. (A) Action of Bay K 8644 ($3 \mu\text{M}$) and (+)-**11** ($3 \mu\text{M}$) applied sequentially to the same cell. Note the marked prolongation of the rising phase of the L-type current induced by (+)-**11** in comparison to the fast activation induced by Bay K 8644. The two currents reach nearly the same maximum value at the end of the pulse and produce identical tail currents on return to -40 mV , suggesting that both compounds produce an equal enhancing effect after about 60–80 ms. The pulse protocol is indicated below. (B) Current/voltage (I/V) characteristics at control and with either $3 \mu\text{M}$ (\pm)-**11** or $3 \mu\text{M}$ Bay K 8644 measured by ramp commands of 1.4 V/s slope. To the left is reported the dose dependence of the voltage shifts produced by increasing doses of (\pm)-**11**. The shifts in millivolts were calculated at the half-maximal current amplitude of the I/V curves in the voltage region of negative slope. (C) Action of $3 \mu\text{M}$ (+)-**11** on L-type currents at potentials between -30 and 0 mV . Note the slow phase of activation at -30 and -20 mV , which becomes progressively faster and more attenuated at -10 and 0 mV . (D) Slowing down of the L-type current induced by (\pm)-**11** is removed by strong conditioning prepulses. The current traces were recorded sequentially with control and during application of (\pm)-**11**. In each case the recordings consisted of two stimulations separated by a 10-s interval in which a test depolarization to -20 mV was preceded (filled circles) or not by a facilitatory prepulse of 50 ms to $+80 \text{ mV}$. Notice the absence of any change of the current kinetics in the control and the complete removal of the current prolongation in the presence of (\pm)-**11**.

action of the racemates was comparable to that of the (+)-enantiomers (middle column) but opposite to that of the corresponding (–)-enantiomers which had little or no antagonist effects (right column).

Of the compounds tested, the benzofurazan derivative (\pm)-**11** and its enantiomer (+)-**11** were by no means the most potent molecules of the series studied. They had very similar action with average current increases at -20 mV of $247 \pm 21\%$ ($n = 8$) and $224 \pm 27\%$ ($n = 5$), respectively. The second benzofurazan derivative (\pm)-**10** and its enantiomer (+)-**10** produced much smaller current enhancements ($164 \pm 4\%$, $n = 12$), while the benzofuroxan derivatives (\pm)-**13** and (\pm)-**12** were even less effective and, thus, not further investigated.

An interesting feature of (\pm)-**11** and (+)-**11** was their ability to slow the rate of rise of the L-type current, an effect which has not previously been reported for other well-known DHP agonists, such as Bay K 8644 and 202-791.^{11–13} Direct comparison of the action of (+)-**11** with respect to Bay K 8644 on the same cell clarified how the two DHPs act on L-type current activation (Figure 3A). Bay K 8644 produced a nearly 2–3-fold increase of the control current without significantly altering the

rate of rise of the current, while (+)-**11** caused a net prolongation of the current which had hardly reached a steady-state level by the end of the pulse. It should be noted that Bay K 8644 and (+)-**11** (or (\pm)-**11**) had nearly identical effects on the current/voltage characteristics. They both shifted the current/voltage curve toward more negative potentials (Figure 3B, left). The voltage shift in the ramp of several millivolts was dose-dependent and saturated at concentrations of (\pm)-**11** above $10 \mu\text{M}$ (Figure 3B, right). The origin of the slow activation phase induced by (\pm)-**11** and its enantiomer (+)-**11** on L-type currents was studied in a series of experiments in which the action of the two agonists was tested at increasing voltages (Figure 3C). The slowing down of activation was most evident below -20 mV , while at more positive voltages ($> -10 \text{ mV}$) the slow phase was less pronounced and progressively faster. At -30 mV the slow phase had an average time constant of 26.3 ms (τ_{slow}) and contributed to about 50% of the total DHP-modified current, while at -10 mV the average τ_{slow} was 9.4 ms and contributed to approximately 23% of the total amplitude. At 0 mV there was almost no difference between the rate of rise of the current in the control and with the agonist despite the marked current enhancement. In eight cells τ_{fast} was $1.1 \pm 0.1 \text{ ms}$ in the control and $1.3 \pm 0.1 \text{ ms}$ in the presence of **11**. This “voltage-dependent” modulation of Ca^{2+} channel activation is reminiscent of the modulating effects of G proteins on N-type channels and is generally interpreted as a reversible inhibition of Ca^{2+} channel gating.¹⁴ The opening of N-type channels is markedly delayed at negative membrane potential, but the delay is progressively removed with increasing positive potential (facilitation),¹⁵ although through different mechanisms of action this seems to hold true also for the “voltage-dependent” effects of (\pm)-**11** (or (+)-**11**) on L-type channels. We tested this by applying the classical double-pulse protocol in which the test pulse to -20 mV is preceded by a strong and brief prepulse to $+80 \text{ mV}$ (Figure 3D). In the absence of the prepulse, the activation of the Ba^{2+} current is markedly delayed with (\pm)-**11**, but the delay is removed following the facilitatory prepulse (filled circle). It should be noted that under control conditions the prepulse does not alter the activation kinetics of Ba^{2+} currents at -20 mV (top traces in Figure 3D).

Discussion

Our data show that enantiomers of methyl 1,4-dihydro-2,6-dimethyl-5-nitro-4-(benzofurazanyl)pyridine-3-carboxylates **10** and **11** and their benzofuroxanyl analogues **12** and **13** display opposite effects on Ca^{2+} currents through voltage-dependent L-type calcium channels. Dextrorotatory antipodes are potent calcium entry activators, while the levorotatory ones are weak calcium entry blockers. Consequently the corresponding racemic mixtures behaved preferentially as Ca^{2+} agonists. Noteworthy is the behavior of the racemic mixture of derivative (\pm)-**11** and its (+)-enantiomer, which was the most potent of the series. This compound, besides causing a potentiation of L-type currents, is capable of interfering with the voltage-dependent gateings of L-type channels, by producing a net delay in the channel activation. To our knowledge, this latter property was observed and only partially described for the 4-(2-

benzylbenzoyl)-2,5-dimethyl-1*H*-pyrrole-3-carboxylic acid methyl ester (FPL 64176), an L-type Ca^{2+} channel activator with a benzoylpyrrole structure.¹⁶ The racemate (\pm)-**10** and its (+)-enantiomer do not display this activity. This suggests that in **11** the benzofurazan-5-yl moiety could interact with a receptor region, near the area fitted by the 1,4-dihydropyridine substructure, which cannot be occupied by the benzofurazan-4-yl substructure in **10**. Although in **13** the benzofuroxan ring is properly oriented to interact with the same receptor region fitted by benzofurazan in **11**, this former compound exerts a strongly reduced capacity to alter the rate constant of Ca^{2+} channel activation. Benzofurazan and benzofuroxan rings have similar lipophilicity ($\log P = 1.62$ and 1.43 , respectively),¹⁷ but different electronic distribution, as evidenced by their ¹H NMR spectra.¹⁸ Thus we can hypothesize that in **11** the correct orientation of the benzofurazan system and/or its electronic properties are important determinants in slowing down the rate of L-type current rise. Probably, these two characteristics are crucial for the interactions of **11** with the gating charges which control the voltage-dependent transition of L-type Ca^{2+} channels from their closed to open conformation.¹⁹ Anyway, at this stage of our work, it is difficult to draw more precise conclusions about structure–activity relationships, owing to the limited number of structures studied.

In conclusion the results of the present work open up interesting issues concerning the utility of these molecules for probing Ca^{2+} channel structure. In addition they uncover the possibility to design new 1,4-DHPs with potential utility as therapeutical tools in the treatment of pathologies where a modest selectivity and a significant use-dependent agonistic action on these channels would be beneficial.

Experimental Section

Melting points were determined on a Büchi 530 apparatus after introducing the sample into the bath at a temperature 10 °C lower than the melting point. A heating rate of 1 °C min^{-1} was used, 3 °C min^{-1} in the case of decomposition. The compounds were routinely checked by infrared spectrophotometry (Shimadzu FT-IR 8101 M). ¹H and ¹³C NMR spectra were recorded on a Bruker AC-200 spectrometer. Resonance assignments were given by analyzing the spectra at low temperature to resolve averaged signals of the two tautomers **13a,b** and **12a,b**, respectively. Column chromatography was performed on silica gel (Merck Kieselgel 60, 230–400 mesh ASTM) with the indicated solvent system. Anhydrous MgSO_4 was used as drying agent. Solvent removal was achieved under reduced pressure at room temperature. Elemental analyses of the new compounds were performed by REDOX (Cologno M.) and the results are within $\pm 0.4\%$ of the theoretical values. Intermediates **1**,⁵ **2**,⁵ **5**,⁵ and **6**²⁰ were synthesized according to the literature. HPLC studies on Chiralpak AS (Daicel Co., Tokyo) were performed with a Merck-Hitachi Lichrograph model L-600 HPLC pump at controlled temperature 22 °C, a Merck-Hitachi Lichrograph L-4000 UV detector ($\lambda = 254$ nm), and a Merck D-2500 recorder. Dead volume was determined by co-injection of 1,3,5-tri-*tert*-butylbenzene. Two columns were used, one (250 \times 4.6 mm) for analytical purposes and one (250 \times 10 mm) for semipreparative applications. Specific rotations were measured on a Perkin Elmer 241 polarimeter.

Cell Culture and Solutions. RINm5F cells were kindly provided by Dr. E. Sher (Eli Lilly and Co., Windlesham, Surrey, U.K.) and were cultured as previously described.⁹ The recording external solution was (mM) 135 NaCl, 10 BaCl_2 , 1 MgCl_2 , 10 HEPES (pH 7.3 with NaOH), and 300 nM TTX. The standard internal solution was (mM) 110 CsCl, 30 TEACl, 10

EGTA, 8 glucose, 10 HEPES, 2 Mg-ATP, 0.25 cAMP, 0.5 GTP, and 15 phosphocreatine (pH 7.3 with CsOH). The four racemates and their enantiomers as well as Bay K 8644 (Bayer AG, Wuppertal, Germany) were dissolved in ethanol (95%) and stored in the dark at 4 °C as 1 mM stock solutions. Dilution to the final concentration was performed daily under light protection. The external solutions were exchanged by fast superfusion using a multibarrelled glass pipet held close to the cell.²¹ Experiments were carried out at room temperature (22 °C).

Whole-Cell Current Recordings. Membrane currents were measured in the whole-cell configuration using a List EPC7 (Darmstadt, Germany) patch-clamp amplifier and pipets of borosilicate glass with a resistance of 3–4 M Ω . Stimulation, acquisition, filtering, and data analysis were performed as described elsewhere.¹⁰ Cells were clamped at -60 mV holding potential (V_h). Step depolarizations of 60–150 ms from V_h were applied at intervals of 10 s to minimize Ca^{2+} channel “rundown”. Capacitative and leakage currents were compensated electronically and by subtracting residual Cd^{2+} -insensitive currents remaining after addition of 200 μM Cd^{2+} . Data are expressed as means \pm SEM for $n =$ number of cells.

General Method of Preparation of DHPs 10, 11, and 13. A solution of the appropriate aldehyde (Scheme 1: **1**, **2**, **5**) (5 mmol) and nitroacetone (**4**) (0.62 g, 6 mmol) in 2-propanol (15 mL) was refluxed for 1 h and then methyl 3-aminocrotonate (**3**) (0.58 g, 5 mmol) was added. Reflux was continued for 5 h. Solvent removal gave a residue, which was purified by flash chromatography. Chromatographic eluents, yields, melting points, and crystallization solvents of the products were as follows.

(\pm)-Methyl 1,4-dihydro-2,6-dimethyl-5-nitro-4-(benzofurazan-4-yl)pyridine-3-carboxylate (**10**): eluent $\text{CH}_2\text{Cl}_2/\text{EtOAc}$ (95/5, v/v); yield 40%; mp 208–209 °C ($\text{EtOAc}/\text{petroleum ether}$ 40–60 °C) (lit. mp 205 °C);²² ¹H NMR (CD_3COCD_3) δ 5.85 (s, 1H, CH-4), 2.55/2.34 (2s, 6H, 2- $\text{CH}_3/6\text{-CH}_3$), 3.59 (s, 3H, OCH_3), 8.92 (br s, 1H, NH), 7.81–7.48 (m, 3H, Arom). Anal. ($\text{C}_{15}\text{H}_{14}\text{N}_4\text{O}_5$) C, H, N.

(\pm)-Methyl 1,4-dihydro-2,6-dimethyl-5-nitro-4-(benzofurazan-5-yl)pyridine-3-carboxylate (**11**): eluent $\text{CH}_2\text{Cl}_2/\text{EtOAc}$ (95/5, v/v); yield 35%; mp 171–172 °C ($\text{EtOAc}/\text{petroleum ether}$ 40–60 °C); ¹H NMR (CD_3COCD_3) δ 5.60 (s, 1H, CH-4), 2.71/2.53 (2s, 6H, 2- $\text{CH}_3/6\text{-CH}_3$), 3.77 (s, 3H, OCH_3), 8.96 (br s, 1H, NH), 7.98–7.74 (m, 3H, Arom). Anal. ($\text{C}_{15}\text{H}_{14}\text{N}_4\text{O}_5$) C, H, N.

(\pm)-Methyl 1,4-dihydro-2,6-dimethyl-5-nitro-4-(benzofuroxan-5(6)-yl)pyridine-3-carboxylate (**13**): eluent petroleum ether 40–60 °C/ EtOAc (7/3, v/v); yield 35%; mp 159–160 °C dec ($\text{EtOAc}/\text{petroleum ether}$ 40–60 °C); ¹H NMR (CD_3COCD_3) δ for **13a,b** 5.32/5.30 (s, 1H, CH-4), 2.56, 2.57/2.38, 2.38 (2s, 6H, 2- $\text{CH}_3/6\text{-CH}_3$), 3.63/3.64 (s, 3H, OCH_3), 9.14/9.11 (br s, 1H, NH), 7.23–7.60/7.23–7.60 (Arom). Anal. ($\text{C}_{15}\text{H}_{14}\text{N}_4\text{O}_6$) C, H, N.

2-Azido-3-nitrobenzaldehyde (8). Concentrated sulfuric acid (330 mL) was added dropwise to a mechanically stirred and ice–salt-cooled solution of **6** (25 g, 0.14 mol) in a mixture of acetic acid (200 mL) and acetic anhydride (200 mL), keeping the temperature below 20–25 °C. The mixture was cooled below 10 °C, and then CrO_3 (39 g, 0.39 mol) was added portionwise, keeping the temperature below 10 °C. After this addition the mixture was stirred, without any control of temperature, for 3 h and then poured into ice–water. The resulting yellow precipitate was collected by filtration, washed with water, then treated with a 2% Na_2CO_3 solution, and again filtered and washed with water. The crude product was partially purified by crystallization ($\text{EtOH}/\text{H}_2\text{O}$) to obtain **7** (40%) sufficiently pure to be used for further reaction. Hydrolysis of **7** (17 g) in a boiling mixture of water (100 mL), EtOH (50 mL), and concentrated hydrochloric acid (75 mL) afforded after 45 min the title product: yield 75%; mp 60–61 °C dec (EtOH/water) (lit.²³ mp 60–61 °C).

(\pm)-Methyl 1,4-dihydro-2,6-dimethyl-5-nitro-4-(2-azido-3-nitrophenyl)pyridine-3-carboxylate (**9**): prepared and purified according to the method described for the preparation

of the analogues **10**, **11**, and **13**; eluent CH₂Cl₂/EtOAc (95/5, v/v); yield 28%; mp 188–190 °C dec (EtOAc/petroleum ether 40–60 °C); ¹H NMR (DMSO-*d*₆) δ 5.69 (s, 1H, CH-4), 2.31 (2s, 6H, 2-CH₃/6-CH₃), 3.59 (s, 3H, OCH₃), 9.78 (br s, 1H, NH), 7.97–7.41 (m, 3H, Arom). Anal. (C₁₅H₁₄N₆O₆) C, H, N.

(±)-Methyl 1,4-Dihydro-2,6-dimethyl-5-nitro-4-(benzofuroxan-4(7)-yl)pyridine-3-carboxylate (**12**). A solution of **9** (0.56 g) in distilled THF (50 mL) in a quartz vessel was irradiated under nitrogen for 24 h with a medium-pressure Hg lamp in an immersion well Rayonet-type photochemical apparatus. The solution was then concentrated, and 2 N hydrochloric acid (10 mL) was added. The resulting mixture was stirred for 20 min at room temperature; the organic phase was separated, dried, and evaporated. The residue was purified by flash chromatography: eluent petroleum ether 40–60 °C/THF (7/3, v/v); yield 40%; mp 153–158 °C dec (THF/petroleum ether 40–60 °C); ¹H NMR (CD₃COCD₃) δ for **12a,b** 5.77/5.99 (s, 1H, CH-4), 2.52, 2.52/2.33, 2.36 (2s, 6H, 2-CH₃/6-CH₃), 3.60/3.46 (s, 3H, OCH₃), 9.01/8.76 (br s, 1H, NH), 7.24–7.55/7.24–7.55 (m, 3H, Arom). Anal. (C₁₅H₁₄N₄O₆) C, H, N.

HPLC Separation of Racemic Mixtures (±)-10, (±)-11, (±)-12, and (±)-13. HPLC separation was performed on a semipreparative Chiralpak AS column (25 × 1 cm); eluent hexane/ethanol (85/15); flow rate 3 mL/min, *t*₀ = 4.7 min: **10** *k*(–) 1.68, [α]²⁵_D = +37 (*c* = 0.50, EtOH), mp 205 °C, *k*(+) 2.04, [α]²⁵_D = –36 (*c* = 0.55, EtOH), mp 205 °C, α = 1.22, Res = 0.66; **11** *k*(–) 1.77, [α]²⁵_D = +11 (*c* = 0.40, EtOH), mp 170–171 °C, *k*(+) 2.62, [α]²⁵_D = –11 (*c* = 0.40, EtOH), mp 170–171 °C, α = 1.48, Res = 1.3; **12** *k*(–) 3.09, [α]²⁵_D = +36.2 (*c* = 0.50, EtOH), mp 152–158 °C dec, *k*(+) 3.78, [α]²⁵_D = –38.2 (*c* = 0.47, EtOH), mp 152–158 °C dec, α = 1.23, Res = 0.9; **13** *k*(–) 3.45, [α]²⁵_D = +8.18 (*c* = 0.55, EtOH), mp 159–160 °C dec, *k*(+) 5.19, [α]²⁵_D = –8.19 (*c* = 0.55; EtOH), mp 159–160 °C dec, α = 1.50, Res = 1.1.

Acknowledgment. This work was supported by a MURST grant.

References

- Triggle, D. J.; Langs, D. A.; Janis, R. A. Ca²⁺ Channel Ligands: Structure–Function Relationships of the 1,4-Dihydropyridines. *Med. Res. Rev.* **1989**, *9*, 123–180.
- Goldmann, S.; Stoltefuss, J. 1,4-Dihydropyridines: Effects of Chirality and Conformation on the Calcium Antagonist and Calcium Agonist Activities. *Angew. Chem., Int. Ed. Engl.* **1991**, *30*, 1559–1578.
- Rovnyak, G. C.; Kimball, S. D.; Beyer, B.; Cucinotta, G.; Di Marco, J. D.; Gougoutas, J.; Hedberg, A.; Malley, M.; McCarthy, J. P.; Zhang, R.; Moreland, S. Calcium Entry Blockers and Activators: Conformational and Structural Determinants of Dihydropyridine Calcium Channel Modulators. *J. Med. Chem.* **1995**, *38*, 119–129.
- Vo, D.; Matowe, W. C.; Ramesh, M.; Iqbal, N.; Wolowyk, M. W.; Howlett, S. E.; Knaus, E. E. Modulation Activities, and Voltage-Clamp Studies of Isopropyl 1,4-Dihydro-2,6-dimethyl-3-nitro-4-pyridine-5-carboxylate Racemates and Enantiomers. *J. Med. Chem.* **1995**, *38*, 2851–2859.
- Gasco, A. M.; Ermondi, G.; Fruttero, R.; Gasco, A. Benzofurazanyl- and benzofuroxanyl-1,4-dihydropyridines: synthesis, structure and calcium entry blocker activity. *Eur. J. Med. Chem.* **1996**, *31*, 3–10.
- Gasco, A.; Boulton, A. J. Furoxans and Benzofuroxans. In *Advances in Heterocyclic Chemistry*; Katritzky, A. R., Boulton, A. J., Eds.; J. Wiley: New York, 1981; Vol. 29, pp 251–340.
- Boulton, A. J.; Halls, P. J.; Katritzky, A. R. *N*-Oxides and Related Compounds. Part XXXVII. The effect of Methyl and Aza-substituents on the Tautomeric Equilibrium in Benzofuroxan. *J. Chem. Soc. B* **1970**, 636–640. Boulton, A. J.; Katritzky, A. R.; Swell, M. J.; Wallis, B. *N*-Oxides and Related Compounds. Part XXXI. The Nuclear Magnetic Resonance Spectra and Tautomerism of Some Substituted Benzofuroxans. *J. Chem. Soc. B* **1967**, 914–919.
- Chiralpak AS is available from DAICEL Co., Tokyo, Japan.
- Pollo, A.; Lovallo, M.; Biancardi, E.; Sher, E.; Succi, C.; Carbone, E. Sensitivity to dihydropyridines, ω-conotoxin and noradrenaline reveals multiple HVA Ca²⁺ channels in rat insulinoma and human pancreatic β-cells. *Pflügers Archiv.* **1993**, *423*, 462–471.
- Magnelli, V.; Pollo, A.; Sher, E.; and Carbone, E. Block of non-L-, non-N-type Ca²⁺ channels in rat insulinoma RINm5F cells by ω-conotoxin MVIIC. *Pflügers Archiv.* **1995**, *429*, 762–771.
- Sanguinetti, M. C.; Krafte, D. S.; Kass, R. S. Voltage-dependent modulation of Ca²⁺ channel current in heart cells by Bay K 8644. *J. Gen. Physiol.* **1986**, *88*, 369–392.
- Kokubun, S.; Prod'homme, B.; Becker, C.; Porzig, H.; Reuter, H. Studies on Ca²⁺ channels in intact cardiac cells: voltage-dependent effects and cooperative interactions of dihydropyridine enantiomers. *Mol. Pharmacol.* **1986**, *30*, 571–584.
- Brown, A. M.; Kunze, D. L.; Yatani, A. The agonist effect of dihydropyridines on Ca²⁺ channels. *Nature* **1984**, *311*, 570–572.
- Carbone, E.; Magnelli, V.; Pollo, A.; Carabelli, V.; Albillos, A.; Zucker, H. Biophysics of voltage-dependent Ca²⁺ channels: gating kinetics and their modulation. In *Ion Channel Pharmacology*; Soria, B., Ceña, V., Eds.; Oxford University Press: Oxford, England, 1998; pp 97–128.
- Carabelli, V.; Lovallo, M.; Magnelli, V.; Zucker, H.; Carbone, E. Voltage-dependent modulation of single N-type channel kinetics by receptor agonists in IMR32 cells. *Biophys. J.* **1996**, *70*, 2144–2154.
- Rampe, D.; Anderson, B.; Rapien-Pryor, V.; Li, T.; Dage, R. C. *J. Pharmacol. Exp. Ther.* **1993**, *265*, 1125–1130.
- Calvino, R.; Gasco, A.; Leo, A. An Analysis of Lipophilicity of Furazan and Furoxan Derivatives using the CLOGP Algorithm. *J. Chem. Soc., Perkin Trans.* **1992**, *2*, 1643–1646.
- Harris, R. K.; Katritzky, A. R.; Øksne, S.; Bailey, A. S.; Paterson, W. G. *N*-Oxides and Related Compounds. Part XIX. Proton Resonance Spectra and the Structure of Benzofuroxan and its Nitro-derivatives. *J. Chem. Soc.* **1963**, 197–203.
- Armstrong, C. M.; Hille, B. Voltage-gated ion channels and electrical excitability. *Neuron* **1998**, *20*, 371–380.
- Zincke, T.; Schwarz, P. Über *o*-Dinitroverbindungen der Benzolreihe. *Ann. Chem.* **1899**, *307*, 28–49.
- Carbone, E.; Lux, H. D. Kinetics and selectivity of a low voltage-activated calcium current in chick and rat sensory neurones. *J. Physiol.* **1987**, *386*, 547–570.
- Vogel, A.; Bormann, G. Nouveaux Dérivés de la 1,4-Dihydropyridine, Leur Préparation et leur Utilisation en Thérapeutique Comme Médicaments. BE 900874, 1985.
- Balasubrahmanyam, S. N.; Radhakrishna, A. S.; Boulton, A. J.; Kan-Woon, T. Furazans and Furazan Oxides. 7. Interconversion of Anthranils, Benzofurazan Oxides, and Indazoles. *J. Org. Chem.* **1977**, *42*, 897–901.

JM980623B